Tunable photonic band gaps in two-dimensional photonic crystals by temporal modulation based on the Pockels effect

Hiroyuki Takeda and Katsumi Yoshino
Department of Electronic Engineering, Graduate School of Engineering, Osaka University, 2-1 Yamada-Oka, Suita, Osaka 565-0871, Japan
(Received 23 February 2003; published 27 January 2004)

We theoretically demonstrate the tuning of photonic band gaps in two-dimensional photonic crystals composed of rods by temporal modulation based on the Pockels effect. Refractive indices of rods can be changed periodically by applied alternating voltage under the influence of the Pockels effect, which causes new photonic band states other than original ones. Therefore, photonic band gaps can be closed by the new photonic band states, which may provide novel applications for tunable photonic crystals.

DOI: 10.1103/PhysRevE.69.016605 PACS number(s): 42.70.Qs

I. INTRODUCTION

Recently, photonic crystals have attracted much attention from both fundamental and practical viewpoints, because novel concepts such as photonic band gaps (PBGs) have been predicted, and various new applications of photonic crystals have been proposed [1–3]. In earlier studies, two fundamentally new optical principles, namely, the localization of light [4–6] and the controllable inhibition of spontaneous emission of light [7–10], were considered to be the most important.

For applications in optical devices, on the other hand, it is important to realize the tunability of photonic crystals, that is, to control photonic band structures such as photonic band gaps. Therefore, tunable photonic crystals composed of materials whose properties can be changed by adjusting external factors have been proposed [11–13]. Moreover, for many applications, it is advantageous to obtain tunable photonic crystals through electrooptic effects.

In optical devices, materials whose refractive indices can be changed by applied voltage are widely used. For example, optical properties are temporally modulated by alternating voltage with the Pockels effect in which the change of refractive indices is proportional to applied voltage. It is important to control optical properties via external factors with respect to applications.

Therefore, we propose the use of temporal modulation based on the Pockels effect in photonic crystals. Refractive indices can be changed periodically due to the Pockels effect, by applied alternating voltage which causes new photonic band states which are significantly dependent on magnitudes of changes of refractive indices and modulation frequencies. In general, it is difficult to obtain large tunabilities by changing the refractive indices of materials. In photonic crystals, however, large tunabilities can be obtained by temporal modulation.

In this paper, we theoretically demonstrate the tuning of photonic band gaps in two-dimensional photonic crystals composed of rods with square lattices by temporal modulation based on the Pockels effect. Rods are assumed to be composed of strontium barium niobate (SBN) which is a photorefractive crystal having a very large electrooptical coefficient. Experimentally, it is possible to fabricate photonic crystals of SBN with a thickness of 4.5 μm [14], and therefore we can consider two-dimensional photonic crystals, since the thickness of the photonic crystals is much larger than the lattice constants of light wavelength order [15,16]. Moreover, electrodes are assumed to be attached at the top and bottom of crystals in order to apply electric field. However, we neglect the effects of electrodes on photonic crystals because of the long thickness of crystals in comparison with light wavelength order. We treat the transversal magnetic (TM) mode, because the photonic crystal has large photonic band gaps in the case of the TM mode. Moreover, the c axis of SBN is assumed to be parallel to the rods, and then, the electric field of the electromagnetic waves parallel to rods has extraordinary refractive indices. Alternating voltage is applied in the direction parallel to the rods. We assume large modulation frequencies in order to achieve effective tunabilities.

II. THEORY

Unlike conventional photonic crystals, the dielectric constant of a rod $\epsilon(t)$ depends on time in temporal modulation based on the Pockels effect. $\epsilon(t)$ is represented as

$$\begin{aligned}\epsilon(t) &= (n_e + \Delta n_e(t))^2 \\ &= n_e^2 + 2n_e \Delta n_e(t) + \Delta n_e(t)^2 \\ &\sim n_e^2 + 2n_e \Delta n_e(t) \quad [\Delta n_e(t)/n_e \ll 1] \\ &= n_e^2 + n_e^4 \gamma_{33} E_m \sin \Omega t \\ &= \epsilon_c + \delta\epsilon \sin \Omega t \quad (\epsilon_c = n_e^2, \delta\epsilon = n_e^4 \gamma_{33} E_m), \end{aligned} \tag{1}$$

where n_e, $\Delta n_e(t)$, γ_{33}, E_m and Ω are the extraordinary refractive index, the change of the refractive index, the electrooptical coefficient, the maximum applied electric field, and the modulation frequency, respectively.

In order to obtain photonic band structures and transmission spectra of two-dimensional photonic crystals composed of rods with square lattices, we perform calculations using

the finite difference time domain (FDTD) method [17]. Electromagnetic fields $\mathbf{E}(\mathbf{r},t)$ and $\mathbf{H}(\mathbf{r},t)$ satisfy the following equations:

$$\nabla\times\mathbf{E}(\mathbf{r},t)=-\mu_0\frac{\partial\mathbf{H}(\mathbf{r},t)}{\partial t}, \tag{2a}$$

$$\begin{aligned}\nabla\times\mathbf{H}(\mathbf{r},t)&=\epsilon_0\frac{\partial\epsilon(\mathbf{r},t)\mathbf{E}(\mathbf{r},t)}{\partial t}\\&=\epsilon_0\frac{\partial\epsilon(\mathbf{r},t)}{\partial t}\mathbf{E}(\mathbf{r},t)+\epsilon_0\epsilon(\mathbf{r},t)\frac{\partial\mathbf{E}(\mathbf{r},t)}{\partial t}\\&=\sigma(\mathbf{r},t)\mathbf{E}(\mathbf{r},t)+\epsilon_0\epsilon(\mathbf{r},t)\frac{\partial\mathbf{E}(\mathbf{r},t)}{\partial t},\end{aligned}$$

$$\left(\sigma(\mathbf{r},t)=\epsilon_0\frac{\partial\epsilon(\mathbf{r},t)}{\partial t}\right), \tag{2b}$$

where ϵ_0 and μ_0 are the permittivity and permeability of free space, respectively.

Equation (2b) corresponds to the problem of electromagnetic fields in materials with conductivity $\sigma(\mathbf{r},t)$. By using discrete time and lattices according to the Yee algorithm [17], we can obtain the photonic band structures and transmission spectra.

Figure 1(a) shows the schematic diagram of a rod in a unit cell of a photonic crystal with a two-dimensional periodicity. R and a indicate the radius of a rod and a lattice constant, respectively. In this system, the initial point source can be set arbitrarily, and the point source and the detector are set at $(0.75a,0.25a)$ and $(0.25a,0.75a)$, respectively, in each unit cell. Bloch's boundary conditions are applied to four edges of the unit cell [18]. In calculating photonic band structures, Bloch's boundary conditions are

$$\mathbf{E}(\mathbf{r}+\mathbf{R},t)=\exp(i\mathbf{k}\cdot\mathbf{R})\mathbf{E}(\mathbf{r},t) \tag{3a}$$

and

$$\mathbf{H}(\mathbf{r}+\mathbf{R},t)=\exp(i\mathbf{k}\cdot\mathbf{R})\mathbf{H}(\mathbf{r},t), \tag{3b}$$

where $\mathbf{k}$ and $\mathbf{R}$ are the wave vector and the lattice vector, respectively. In fact, the wave vector in Bloch's theorem is the equivalent of the crystal momentum in solid-state physics, and for photonic band diagrams, this is a vector pointing toward the boundary of the irreducible part in the first Brillouin zone. For certain wave vectors, the frequency components can be obtained by the Fourier transform of the electric field at the detector when the Gaussian pulse is excited at the point source, as shown in Fig. 1(a). Fourier amplitudes of the Gaussian pulse $\exp(-\{(t-T)/0.29T\}^2)$ $(T=0.646\times 2\pi/\omega_0,\ \omega_0 a/2\pi c=10)$ considered in this paper are constant in the frequency ranges of interest.

The Fourier transform of the electric flux density $\mathbf{D}(\omega)$ is represented as

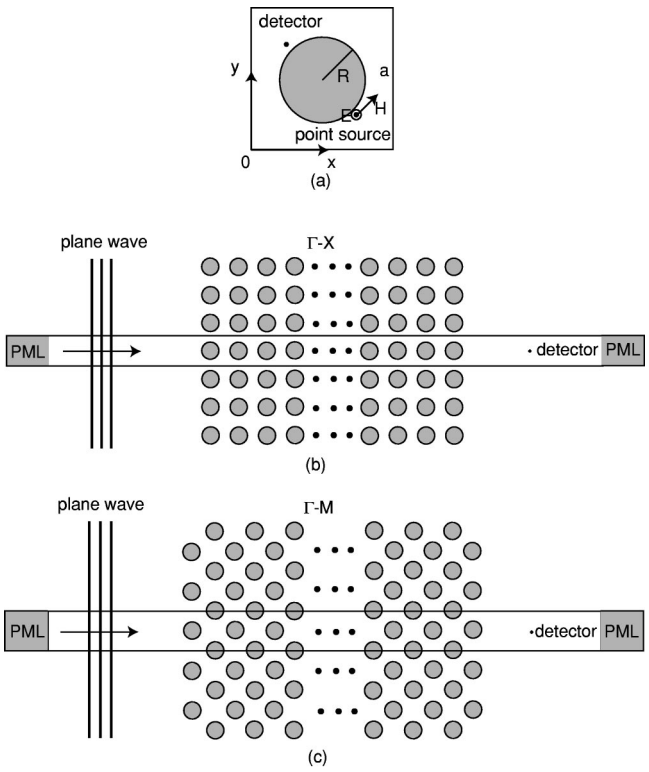

FIG. 1. (a) Schematic diagram of a rod in a unit cell. R and a indicate the radius of a rod and a lattice constant, respectively. The point source and detector are set at $(0.75a,0.25a)$ and $(0.25a,0.75a)$, respectively, in each unit cell. (b) and (c) Schematic diagrams in which plane waves are incident on two-dimensional photonic crystals composed of rods with square lattices in the $\Gamma-X$ and $\Gamma-M$ directions, respectively. The regions embedded by solid lines indicate unit cells used for calculating transmission spectra.

$$\begin{aligned}\mathbf{D}(\omega)&=\int_{-\infty}^{\infty}\epsilon(t)\mathbf{E}(t)\exp(-i\omega t)dt\\&=\epsilon_c\int_{-\infty}^{\infty}\mathbf{E}(t)\exp(-i\omega t)dt\\&\quad+\delta\epsilon\int_{-\infty}^{\infty}\sin\Omega t\mathbf{E}(t)\exp(-i\omega t)dt\\&=\epsilon_c\mathbf{E}(\omega)+\frac{\delta\epsilon}{2i}\{\mathbf{E}(\omega-\Omega)-\mathbf{E}(\omega+\Omega)\},\end{aligned} \tag{4}$$

where $\mathbf{E}(\omega)$ is the Fourier transform of the electric field $\mathbf{E}(t)$. Therefore, new frequency components $\omega\pm\Omega$ appear other than the original frequency component ω in photonic crystals whose refractive indices change temporally.

Figures 1(b) and 1(c) show that plane waves are incident on two-dimensional photonic crystals composed of rods with square lattices in the $\Gamma-X$ and $\Gamma-M$ directions, respectively. The regions embedded by solid lines indicate unit cells used for calculating transmission spectra. When plane waves with the Gaussian pulse are incident on photonic crystals, transmittances can be obtained by the Fourier transform

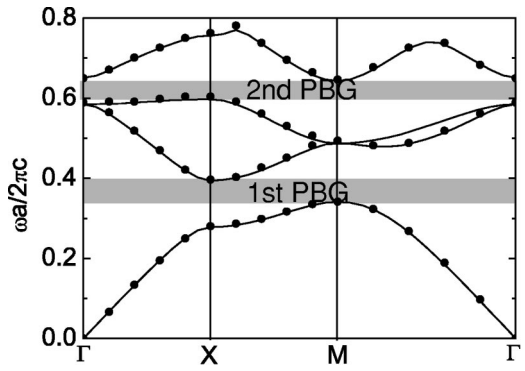

FIG. 2. Photonic band structure in the two-dimensional photonic crystal composed of rods with square lattices. The black point and the solid line indicate the photonic band structures calculated by the FDTD method and the plane wave expansion method, respectively. The extraordinary refractive index is $n_e = 2.3117$, and the radius of a rod is $R/a = 0.3$.

of the electric field at the detector. The sizes of photonic crystals in Figs. 1(a) and 1(b) are 17 and 21 layers, respectively. In calculating transmission spectra, the periodic boundary conditions are satisfied for boundaries parallel to the incident direction of plane waves. On the other hand, perfect matched layers (PML) are satisfied for boundaries perpendicular to the incident direction of plane waves in order to obtain high accuracy in the reflection of electromagnetic waves.

III. NUMERICAL CALCULATION AND DISCUSSION

We calculate the photonic band structure in a two-dimensional photonic crystal composed of rods with square lattices in the case that alternating voltage is not applied. The extraordinary refractive index is $n_e = 2.3117$, and the radius of a rod is $R/a = 0.3$. A background is the air. Figure 2 shows the photonic band structure in the two-dimensional photonic crystal. The black point and the solid line indicate the photonic band structures calculated by the FDTD method and the plane wave expansion method, [19] respectively. In the FDTD method, higher accuracies and stabilities are obtained with increasing discrete time and lattices. The discrete time and lattices are $c\Delta t/a = 0.01$ and $\Delta x/a = \Delta y/a = 0.025$, respectively. These parameters satisfy $c\Delta t \leqslant \{(1/\Delta x)^2 + (1/\Delta y)^2\}^{-1/2}$, which compensates the calculational stability. The number of time steps in this calculation is 50000, and errors are within 1%. In the plane wave method, on the other hand, errors of photonic band structures with 961 plane waves are also within 1%. These calculational results are almost the same. As shown in Fig. 2, there exist two photonic band gaps in the frequency ranges of $(0.341 - 0.394)2\pi c/a$ and $(0.597 - 0.643)2\pi c/a$. We define the former and the latter photonic band gaps as the first and the second photonic band gaps, respectively.

Figure 3(a) shows the Fourier amplitude of the electric field at the X point at $\delta\epsilon/\epsilon_c = 0.0$. As shown in Fig. 3(a), for example, photonic band structures are obtained by investigating some frequency peaks for certain wave vectors. Next, we investigate photonic band structures in the case that alternating voltage is applied. The electrooptical coefficient of SBN is $\gamma_{33} = 1340$ pm/V. We assume that the maximum change of the dielectric constant is $\delta\epsilon/\epsilon_c = 0.1$, for simplicity, which can be realized by the maximum applied electric field $E_m = 1.4 \times 10^7$ V/m. Photonic band structures are different from the original ones when alternating voltage is applied. Figure 3(b) shows the Fourier amplitude of the electric field at the X point at $\delta\epsilon/\epsilon_c = 0.1$ and $\Omega a/2\pi c = 0.027$. As shown in Fig. 3(b), some new frequency peaks appear at both sides of the original peaks, and the interval between the original and new frequency peaks is Ω, which originates from temporal modulation, as mentioned in Eq. (4).

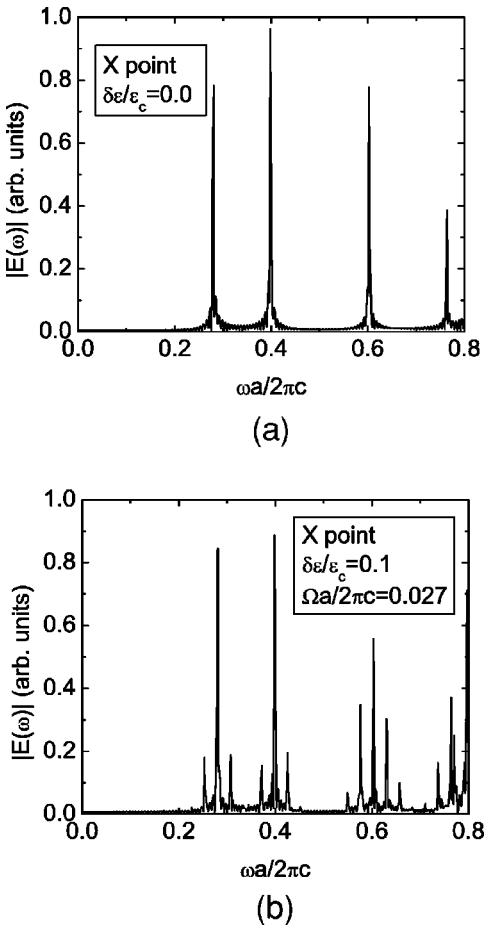

FIG. 3. Fourier amplitude of the electric field at the X point at (a) $\delta\epsilon/\epsilon_c = 0.0$ and (b) $\delta\epsilon/\epsilon_c = 0.1$ and $\Omega a/2\pi c = 0.027$.

We investigate the intensity of the new frequency peak relative to that of the original frequency peak of the first band at the X point. Figure 4(a) shows the dependence of $|E(\omega+\Omega)/E(\omega)|$ of the first band at the X point on $\delta\epsilon/\epsilon_c$ ranging from 0 to 0.1 at $\Omega a/2\pi c = 0.027$. As shown in Fig. 4(a), $|E(\omega+\Omega)/E(\omega)|$ increases monotonically with increasing $\delta\epsilon/\epsilon_c$. On the other hand, Fig. 4(b) shows the dependence of $|E(\omega+\Omega)/E(\omega)|$ of the first band at the X point on $\Omega a/2\pi c$ ranging from 0.01 to 0.04 at $\delta\epsilon/\epsilon_c = 0.1$. As evident in Fig. 4(b), $|E(\omega+\Omega)/E(\omega)|$ decreases with increasing $\Omega a/2\pi c$ although it exhibits complex behaviors. That is, the intensities of the new frequency peaks increase

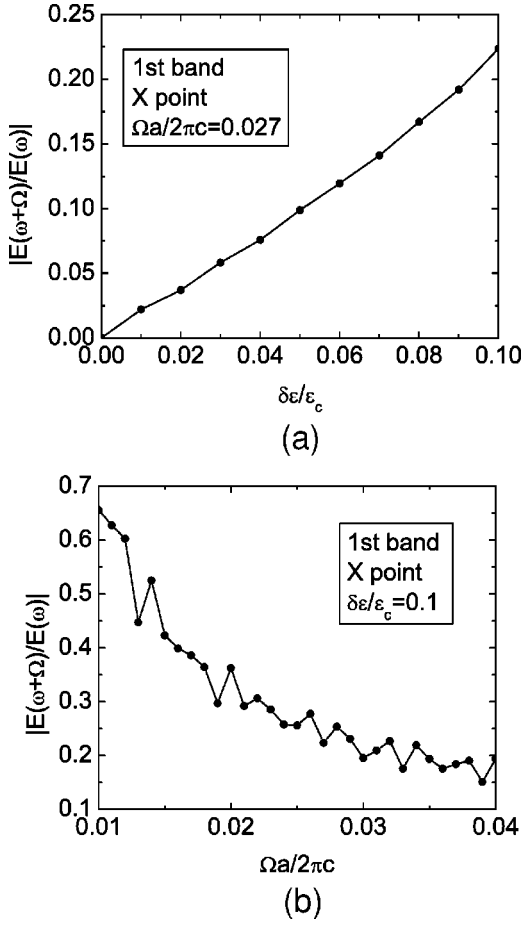

FIG. 4. Dependence of $|E(\omega+\Omega)/E(\omega)|$ of the first band at the X point (a) on $\delta\epsilon/\epsilon_c$ ranging from 0 to 0.1 at $\Omega a/2\pi c=0.027$ and (b) on $\Omega a/2\pi c$ ranging from 0.01 to 0.04 at $\delta\epsilon/\epsilon_c=0.1$.

as $\delta\epsilon/\epsilon_c$ and $\Omega a/2\pi c$ become larger and smaller, respectively.

By utilizing these properties, we can obtain large tunabilities, that is, tunable photonic band gaps. As shown in Fig. 2, for example, the first photonic band gap is decided by the photonic band states of the first band at the M point and the second band at the X point. We define the frequencies of the photonic band states of the first band at the M point and the second band at the X point as ω_M^{1st} and ω_X^{2nd}, respectively. In the first photonic band gap in Fig. 2, new frequency peaks appear at $\omega_M^{1st}+\Omega$ and $\omega_X^{2nd}-\Omega$ when alternating voltage is applied, and the magnitude of the first photonic band gap changes from $\Delta\omega^{1st}=\omega_X^{2nd}-\omega_M^{1st}$ to $\Delta\omega^{1st}-2\Omega$. Therefore, the first photonic band gap is closed by selecting the modulation frequency $\Omega\geqslant\Delta\omega^{1st}/2$. The same concept is also applicable to the second photonic band gap. The magnitudes of the first and the second photonic band gaps are $\Delta\omega^{1st}a/2\pi c=0.053$ and $\Delta\omega^{2nd}a/2\pi c=0.046$, respectively. We select $\Omega a/2\pi c=0.027$ which satisfies $\Omega\geqslant\Delta\omega^{1st,2nd}/2$.

As mentioned above, the new frequency peaks are weaker than the original ones, that is, the transmission spectra originating from the new frequency peaks are also lower. Thus, we calculate transmittances by the FDTD method in order to investigate the efficiency of the new frequency peaks. Figure

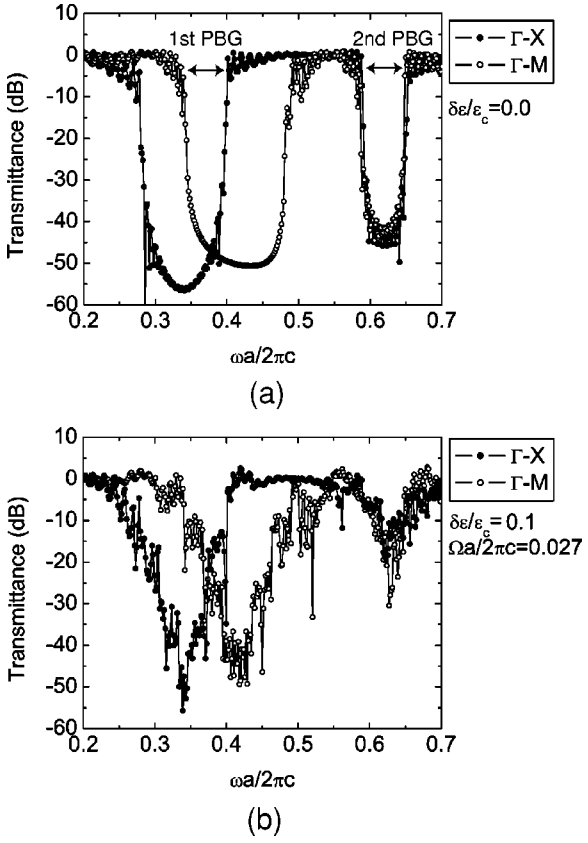

FIG. 5. Transmittances in the $\Gamma-X$ and $\Gamma-M$ directions at (a) $\delta\epsilon/\epsilon_c=0.0$ and (b) $\delta\epsilon/\epsilon_c=0.1$ and $\Omega a/2\pi c=0.027$. The black and white points indicate transmittances in the $\Gamma-X$ and $\Gamma-M$ directions, respectively.

5(a) shows transmittances in the $\Gamma-X$ and $\Gamma-M$ directions at $\delta\epsilon/\epsilon_c=0.0$. The black and white points indicate the transmittances in the $\Gamma-X$ and $\Gamma-M$ directions, respectively. As shown in Fig. 5(a), there exist two photonic band gaps, that is, the first and the second photonic band gaps. In these photonic band gaps, transmittances are lower than -40 (dB). In Fig. 5(b), on the other hand, we show transmittances in the $\Gamma-X$ and $\Gamma-M$ directions at $\delta\epsilon/\epsilon_c=0.1$ and $\Omega a/2\pi c=0.027$. The black and white points indicate the transmittances in the $\Gamma-X$ and $\Gamma-M$ directions, respectively. As shown in Fig. 5(b), there exist no clear photonic band gaps by the new transmittances in the $\Gamma-X$ and $\Gamma-M$ directions, which supports our interpretations. The transmittances become approximately -15 dB in the frequency ranges of the first and the second photonic band gaps in Fig. 5(a). Therefore, we can obtain tunable photonic band gaps in two-dimensional photonic crystals by temporal modulation based on the Pockels effect, which may provide novel applications for tunable photonic crystals. However, it should be noted that the transmittances considered here are time average because of the temporal change of dielectric constants.

IV. CONCLUSION

We theoretically demonstrated the tuning of photonic band gaps by temporal modulation based on the Pockels ef-

fect in two-dimensional photonic crystals composed of rods. Rods are assumed to be composed of strontium barium niobate (SBN) which is a photorefractive crystal having a very large electrooptical coefficient. By changing refractive indices periodically under the influence of applied alternating voltage, some new frequency peaks appear at both sides of the original peaks, and the interval between the original and new frequency peaks is equal to the modulation frequency. Photonic band gaps can be closed by the new photonic band states, which may provide novel applications for tunable photonic crystals.

ACKNOWLEDGMENT

This work was partly supported by a Grant-in-Aid for Scientific Research from the Ministry of Education, Culture, Sports, Science and Technology.

[1] S. John, Phys. Rev. Lett. **58**, 2486 (1987).
[2] E. Yablonovitch, Phys. Rev. Lett. **58**, 2059 (1987).
[3] S. John and T. Quang, Phys. Rev. Lett. **74**, 3419 (1995).
[4] S. John, Phys. Rev. Lett. **53**, 2169 (1984).
[5] A.Z. Genack and N. Garcia, Phys. Rev. Lett. **66**, 2064 (1991).
[6] D. Wiersma, P. Bartolini, A. Lagendijk, and R. Righini, Nature (London) **390**, 671 (1997).
[7] V.P. Bykov, Sov. J. Quantum Electron. **4**, 861 (1975).
[8] S. John and J. Wang, Phys. Rev. Lett. **64**, 2418 (1990).
[9] S. John and T. Quang, Phys. Rev. A **50**, 1764 (1994).
[10] T. Quang, M. Woldeyohannes, S. John, and G.S. Agarwal, Phys. Rev. Lett. **79**, 5238 (1997).
[11] K. Yoshino, Y. Shimoda, Y. Kawagishi, K. Nakayama, and M. Ozaki, Appl. Phys. Lett. **75**, 932 (1999).
[12] K. Busch and S. John, Phys. Rev. Lett. **83**, 967 (1999).
[13] Y. Saado, M. Golosovsky, D. Davidov, and A. Frenkel, Phys. Rev. B **66**, 195108 (2002).
[14] D. Kip, M. Wesner, E. Krätzig, V. Shandarov, and P. Moretti, Appl. Phys. Lett. **72**, 1960 (1998).
[15] Y. Sugimoto, N. Ikeda, N. Carlsson, K. Asakawa, N. Kawai, and K. Inoue, J. Appl. Phys. **91**, 922 (2002).
[16] T. Tada, V.V. Poborchii, and T. Kanayama, Jpn. J. Appl. Phys., Part 1 **38**, 7253 (1999).
[17] A. Taflove and S. C. Hagness, *Computational Electrodynamics: the Finite-Difference Time-Domain Method* (Artech House, Boston, 1995).
[18] A. Chutinan and S. Noda, Phys. Rev. B **62**, 4488 (2000).
[19] K.M. Ho, C.T. Chan, and C.M. Soukoulis, Phys. Rev. Lett. **65**, 3152 (1990).